Single-grain quartz OSL dating of debris flow deposits from Men Tou Gou, south west Beijing, China

Zhao, Qiuyue ; Thomsen, Kristina Jørkov; Murray, A. S.; Wei, Mingjian ; Song, Bo

Published in:
Quaternary Geochronology

Link to article, DOI:
10.1016/j.quageo.2017.06.001

Publication date:
2017

Document Version
Peer reviewed version

Single-grain quartz OSL dating of debris flow deposits from Men Tou Gou, south west Beijing, China

Qiuyue Zhao [1,2*], Kristina Jørkov Thomsen[3], Andrew Sean Murray[4], Mingjian Wei [2], Bo Song[5]

[1]Key Laboratory of Tourism and Resources Environment in Universities of Shandong–Taishan University, 271000 Taian, China

[2]College of Resource Environment and Tourism – Capital Normal University, 100048 Beijing, China

[3]Center for Nuclear Technologies, Technical University of Denmark, DTU Risø Campus, Frederiksborgvej 399, 4000 Roskilde, Denmark

[4]Nordic Laboratory for Luminescence Dating, Department of Geoscience, University of Aarhus, Risø Campus, Frederiksborgvej 399, 4000 Roskilde , Denmark

[5]Beijing Jing Yuan School, 100040 Beijing, China

* Corresponding author: qyzhao@cnu.edu.cn

Abstract

Debris flows in the mountainous regions south west of Beijing, China occur frequently and often result in considerable mass movements with disastrous consequences for human life, infrastructure and agriculture. Obtaining chronological information on such events is important for the prediction of the return frequency of

these debris flows, risk assessment and climate change research. In this project, we use quartz single-grain optically stimulated luminescence (OSL) methods to determine the burial ages of five debris flow samples from the Zhai Tang region ~60 km west of Beijing. OSL characteristics were found to be acceptable despite the low inherent brightness of quartz extracted from these samples. Single-grain thermal transfer was determined to be negligible and beta dose recovery experiments were satisfactory. The quartz single-grain dose distributions strongly indicate that the samples were poorly bleached prior to deposition; relative over-dispersions are larger than 60%. Minimum age modelling indicates that all five samples were deposited within the past few hundred years, indicating that catastrophic debris flows are occurring under the historically-recent land-use pattern.

Keywords

Quartz; Single grain OSL dating; SAR; Debris flow deposits

1 INTRODUCTION

Debris flows are frequent events in mountainous areas; in China they lead to the death of 300-600 people every year and annual losses of ~2 billion yuan (~US$ 300M, Cui et al., 2000). Although catastrophic debris flows are an unavoidable component of the evolution of mountain landforms (Šilhán and Pánek, 2010), their impact can be reduced by quantifying risk in time and space. Fortunately, debris flow deposits provide a record of the size and frequency of debris flows, as well as of other agents of landscape evolution; they can reflect rainfall, terrain and tectonic movements (Cui et al., 1996). In the region of interest in this study, the mountainous area to the west of Beijing, a knowledge of the age of debris flow deposits, coupled with an understanding of the associated formation environment, hydrodynamic

conditions, and environmental evolution would help in the understanding and assessment of the modern environment and contribute to providing estimates of the likelihood of geological disasters. Unfortunately, the interpretation of the debris flow record in terms of return frequency, risk assessment, and related climate change research is limited by the availability of reliable chronological methods; organic material suitable for ^{14}C dating is rare.

Optically Stimulated Luminescence (OSL) has the potential to determine the time elapsed since the last transport and deposition of sediment; this technique measures the time elapsed since energy trapped in crystal structures (e.g. quartz and feldspar) as a result of exposure to natural ionising radiation was last released by exposure to daylight. However, the opportunity for sufficient light exposure during debris flows is limited and thus heterogeneous resetting of the latent OSL signal is expected. Despite this, Lu et al. (2003) used fine-grain (multi-grain aliquots) OSL techniques (infrared stimulated luminescence, IRSL and green stimulated luminescence, GLSL) to date 9 debris flow deposits samples on the Ma Lan platform (south west of Beijing) and concluded that these sediments were deposited ~7-43 ka ago, i.e. before significant anthropogenic influence and likely in a substantially different climate regime; the presence of Holocene ages indicates that at least some resetting had taken place even in such unlikely environments. Nevertheless, application of standard multi-grain OSL techniques to such deposits is likely to result in a significant over-estimation of the true burial age due to averaging effects (e.g. Olley et al., 1998). Thus, in order to identify the population of grains most likely to have been well-bleached (or well–reset) at deposition, the aliquot size must be reduced, ideally to a single grain, and minimum dose modelling applied. Wu et al. (2010) investigated single grains of quartz extracted from modern debris flow deposits in western Taiwan and found that using the lowest 5% of the single-grain doses (Olley et al., 1998) helped to distinguish well-bleached grains from incompletely bleached grains. Zhao et al. (2015) applied the IEU (Internal/External Consistency Criterion, Thomsen et al., 2003; 2007)

minimum dose model to a recent known-age (<25 years) debris flow from a small (~3.9 km^2) catchment ~140 km north of Beijing and to three palaeo-deposits from a sedimentary sequence containing the evidence of multiple flow events. They obtained an age estimate for the youngest sample consistent with the known age, and minimum ages for the older palaeo-deposits suggesting that there were at least 3 major debris flows in that catchment in the last 1000 years.

In the densely populated and mountainous region around Beijing, debris flows have repeatedly led to mortality and significant economic loss (Xie and Cui, 1992). The aim of our study is to lay the foundation for the reconstruction of debris flow activity history in the Beijing region. Because of the likelihood of incomplete bleaching, we use quartz single-grain OSL techniques. Thermal transfer and dose recovery is first investigated and burial doses for five torrent debris flow deposits from the Men Tou Gou District (Beijing) are derived by application of the IEU minimum dose model. The regional implications of the resulting ages are then considered.

2 REGIONAL SETTING AND SITE DESCRIPTION

The study area is situated in the Zhai Tang Zhen, in the Men Tou Gou District, Beijing (39°57′28.21″N, 115°41′35.66″E); samples were taken beside the Ma Lan Gou, a southern seasonal tributary of the Qingshui River (a tributary of Yongding River) (Fig.1). The local geology is dominated by purple and grey sand shale and sandy slate, and the catchment lies in a mid-latitude eastern continental monsoon climate, with frequent rain storms between June and August; this period delivers ~75% of the annual ~677 mm precipitation. Upstream of our sampling site, the Ma Lan Gou channel is ~6 km long, with a catchment area of ~15 km^2 and a relative elevation of ~100 m. The steep terrain combined with intense rainstorms have led to many debris flows in the area in the historical past (Zhao and Dong,1996; Xie et

105 al.,2001), especially the debris flows at Qing Shui and Zhai Tang in 1950, which
106 affected 53 villages; 84 people were killed, 24 seriously injured and >80 houses were
107 destroyed (Hong, 1995).

108 At our site, a road cuts through debris flow facies from Ma Lan Gou (Fig. 1). The
109 exposed section sits on bedrock and is made up primarily of gravel and mixed hybrid
110 units interleaved with sandy silt deposits. The composite section of Fig. 1c is based on
111 four adjacent and laterally-connected exposures, individually illustrated in Fig. 1d.
112 Some fine sand lenses are also present. The hybrid units are poorly sorted, and contain
113 sub-rounded gravel and silty sands, with randomly oriented large clasts. These units
114 are confidently identified as debris flow deposits.

115

116 # 3 EXPERIMENTAL DETAILS

117 ## 3.1 SAMPLING

118 The freshly exposed sections were cut vertically and cleaned. OSL dating samples
119 were collected using 5 cm diameter 25 cm long steel tubes located as shown in Fig. 1.
120 Samples ZT-1, 3 and ZT-4 were taken from the high energy hybrid units, ZT-2 and
121 ZT-5 were taken from the interleaved lower energy sandy silts (see also Table 1). We
122 interpret samples ZT-1, 2, 3 to have been deposited during the early stages of debris
123 flow, and samples ZT-4,5 to have been deposited as the mass movement ceased, or
124 afterwards. Aluminium foil was used to pack and wrap the two ends of the tube to
125 prevent sample mixing during transport. Samples preparation was carried out under
126 subdued red light and material from the two ends of the sampling tubes was removed
127 for dose rate and water content measurement; sediment from the middle part of the
128 sampling tubes was used for D_e estimation (see below).

129

3.2 SAMPLE PREPARATION

The material collected for OSL measurements was firstly wet-sieved to give the 180-250 μm grain size fraction. The grains were then treated with 10% hydrochloric acid (HCl) and 10% hydrogen peroxide (H_2O_2) to remove carbonates and organic matter. Density separation used sodium polytungstate heavy liquid of density 2.58 and 2.70 g cm^{-3} to separate a quartz-rich fraction. To remove the alpha irradiated skin and any remaining feldspar contamination, the quartz fractions were then etched with 40% hydrofluoric acid (HF) for 60 min, and washed in 10% HCl for 40 min to remove any fluoride precipitates. Any remaining feldspar contamination in quartz was checked by infrared (IR) stimulation to confirm that no samples gave a significant IR signal (compared to blue OSL). All samples were re-sieved after chemical treatment to the size fraction 180-250 μm.

3.3 INSTRUMENTATION AND ANALYSIS

All OSL measurements were made using Risø TL/OSL DA-20 readers (Bøtter-Jensen et al., 2003; 2010). Single-grain OSL measurements were made using the Risø single-grain attachment. Luminescence signals were detected using a combination of a bialkali EMI 9235QB photomultiplier tube and a 7.5 mm Hoya U-340 filter. Single grain OSL measurements made use of a 10 mW green Nd:YVO_4 solid diode-pumped laser emitting at 532 nm and providing a power density of ~50 W cm^{-2} (Duller et al., 1999). Arrays of blue (470 nm) LEDs providing a power density of ~40 mW cm^{-2} at the sample position were used in multi-grain measurements. Green laser stimulation was for 0.9 s at 125 °C whereas blue LED stimulation was for 40 s at 125 °C.

For single-grain measurements individual quartz grains (180-250 μm) were loaded into aluminium single-grain measurement discs each containing a 10×10 matrix of grain holes (depth and diameter of 300 μm). For multi-grain measurements,

quartz grains were mounted in a monolayer on 9.7 mm stainless steel discs using silicone oil. Each multi-grain aliquot contained about 150 grains.

Calibrated $^{90}Sr/^{90}Y$ beta sources (~0.1 Gy.s^{-1}) fitted on the Risø TL/OSL-DA-20 readers were used for laboratory irradiations. The dose rates delivered by these beta sources varied by <5% (standard deviation) across the sample area. Correcting for spatial non-uniformity of the sources (Lapp et al., 2012) did not result in significant changes to measured dose or over-dispersion (OD).

The single-aliquot regenerative dose (SAR) procedure (Murray and Wintle, 2000, 2003; Wintle and Murray, 2006) was used for dose estimation. A preheat of 200 °C for 10 s, a cut heat of 180°C, a heating rate of 5 °C s^{-1}, and a 4.5 Gy test dose were used in all dose measurements. The dose response curves consisted of a minimum of three regeneration doses, a zero dose point (i.e. a measurement of recuperation) and a repeat (recycling) point. In addition, each aliquot was checked for feldspar contamination by the measurement of the IR depletion ratio (Duller, 2003). For single-grain measurements, the largest regeneration dose given was 160 Gy; all single-grain doses larger than 160 Gy are derived using extrapolation and these dose estimates are thus likely to be less reliable.

Multi-grain signals were derived from the summation of the initial 0.64 s of stimulation. The immediately following 0.64 s of stimulation was used for background subtraction. Single-grain signals were derived from the summation of the first 0.06 s of the stimulation curves and the last 0.16 s of stimulation was used for background subtraction. Sensitivity-corrected OSL dose-response curves were fitted using a single saturation exponential function, passing through the origin.

Only D_e estimates with a relative uncertainty of the natural test dose signal less than 30% were accepted (s_{Tn} <30%). In addition, dose estimates were accepted only if (i) recycling and IR depletion ratios lay between 0.8 and 1.2 and (ii) sensitivity corrected recuperation signals were consistent with 0 at two standard deviations. No

dose estimates could be derived for ~46% of the otherwise accepted grains, because the sensitivity corrected natural signal was in saturation on the laboratory dose response curve.

These criteria led to the rejection of 99% of the measured single grains. In addition, 54% of the multi-grain aliquots gave sensitivity-corrected natural signals that lay at or above saturation of the laboratory dose-response curve (out of a total of 54 aliquots of sample ZT-1, -2, -4.)

4 DOSE RATES

By their nature, the deposits are very heterogeneous, but every effort was made to take OSL samples at least 10 cm from the nearest large clast, to minimise the risk of significant perturbation of the gamma dose rate. Potentially light-exposed material (~80 g) taken from the ends of the sample tube was ground and homogenized , cast in wax and stored for more than 21 days to ensure equilibrium between ^{226}Ra and ^{222}Rn. The radionuclide concentrations were then measured using calibrated high resolution gamma spectrometers (Murray et al., 1987). Dose rates (Table 1) derived from the radionuclide concentrations of ^{238}U, ^{232}Th and ^{40}K were derived using the conversion factors provided by Guérin et al. (2011), and the cosmic ray contribution is based on Prescott and Hutton (1994). The water content is the average of observed and saturated water content.

5 LUMINESCENCE CHARACTERISTICS

Multi-grain aliquots (~150 grains each) were first measured to assess the suitability of these samples for OSL dating. Fig. 2 shows a normalised OSL decay curve from a multi-grain aliquot from sample ZT-2 (open triangles) and from calibration quartz (filled circles). The latter is known to be fast component dominated (Hansen et al., 2015), and the comparison demonstrates that the OSL signal from ZT-2 is also fast-component dominated. The inset in Fig. 2 shows a typical dose response

curve from multi-grain aliquots, fitted with a single saturating exponential function passing though the origin.

5.1 THERMAL TRANSFER AND DOSE RECOVERY

Single-grain thermal transfer was measured for sample ZT-2 using a preheat of 200 ℃ for 10 s and a cutheat of 180 ℃, by initially bleaching the sample using the blue LEDs twice for 100 s with an intervening pause of 10,000 s. The resulting dose distribution (Fig. 3a) has an arithmetic average dose of 340 ±190 mGy (n=20). The corresponding CAM_{UL} (Arnold et al., 2009) dose is 180 ±160 mGy (CAM_{UL} is used because of the presence of non-positive dose estimates). We then performed three beta dose recovery experiments using sample ZT-1, ZT-3 and ZT-4, respectively (Fig. 3b,c, and d). The grains were loaded into the single-grain discs and bleached as before prior to being given beta doses of 0.9 Gy (ZT-1, N=3000, Fig. 3c), 3 Gy (ZT-3, N=3300, Fig. 3b) and 6 Gy (ZT-4, N=2300, Fig. 3d), respectively. The resulting dose recovery ratios are 0.92 ±0.16 (n=23, OD=51 ±22%, CAM_{UL}), 0.99 ±0.09 (n=24, OD=33 ±7%, CAM) and 0.96 ±0.05 (n=28, OD=17 ±7%, CAM), respectively. We deduce that our chosen SAR protocol is able to measure a laboratory dose given to these samples before any thermal treatment with sufficient accuracy.

If we do not make use of the standard rejection criteria given in section 3.3 (except for s_{Tn}<30%) the corresponding dose recovery ratios are 1.04 ±0.14 (n=27, OD=50 ±16%), 1.02 ±0.07 (n=40, OD=33 ±5%) and 0.96 ±0.05 (n=31, OD=16 ±7%), respectively. We conclude that applying the standard rejection criteria does not significantly change the measured dose or the OD, but these criteria do reduce the accepted grain population by ~20%, on average.

5.2 D_E DISTRIBUTION AND ANALYSIS

A total of >29,000 individual grains (at least 4,800 for each sample, see Table 2) were measured for the five natural samples. After application of the standard rejection criteria, between 0.8 and 1.0% of the grains gave results accepted into the dose distribution and the majority of these grains were only weakly luminescent; the median of the intensity of the test dose signal of the accepted grains was 8.3 Gy^{-1} (summed over the initial 60 ms of stimulation; 273 grains, 5 samples).

The five natural single-grain dose distributions are shown as scatter plots in Fig. 4, where the OSL signals from the natural test dose are plotted against the equivalent dose. The doses range broadly range between 0 and 300 Gy, but note that dose estimates larger than 160 Gy (see section3.3) are derived by extrapolation and are not necessarily accurate. All dose distributions are significantly positively skewed with OD values ranging between 65±10 and 138±29% and a 'leading edge' at low D_e values. This indicates that these samples may not have been completely bleached before deposition and thus that multi-grain analysis may significantly over-estimate the time of the last deposition.

To derive realistic deposition ages, it is very likely that minimum dose modelling must be applied to the natural single-grain dose distributions in order to identify the grains most likely to have been well-bleached at deposition. Here we apply the IEU minimum dose model (Thomsen et al., 2007; Smedley 2015) making use of the results from the thermal transfer and beta dose recovery experiments described in section 5.1 as input parameters, i.e. values of a and b of 0.14±0.09 and 0.35±0.17 Gy, respectively. The grains identified as well-bleached using this approach are shown in Fig. 4 as filled symbols and the derived minimum burial doses D_b are given in Table 2. The relative number of grains identified as well-bleached range between 13 and 50%. The sample expected to be youngest (ZT- 5) has the highest proportion of well-bleached grains.

In the above analysis, we have only included individual dose estimates which pass the standard rejection criteria given in section 3.3, although the dose recovery experiments showed that applying these criteria led to the rejection of ~20% of the grain population without any significant change to measured dose or over-dispersion. If we now consider dose estimates based on all grains with s_{Tn}<30% (i.e. not using other standard rejection criteria), then the average ratio of D_b calculated using grains passing all the rejection criteria to grains only passing s_{Tn}<30% is 0.99±0.04 (n=5 samples), but the average relative uncertainty on individual dose estimates is ~30% larger if all standard rejection criteria are used. Thus, using the all the standard rejection criteria has no impact on the absolute minimum doses determined, but the precision of the minimum dose estimates is decreased. Similar observations have been made by Thomsen et al., (2012), Geach et al. (2015), Guérin et al. (2015b), Hansen et al. (2015), Kristensen et al. (2015), Zhao et al., (2015); Guérin et al. (2016), Thomsen et al., (2016).

Using minimum dose modelling relying on individual uncertainties to derive minimum dose is usually very dependent on the assigned uncertainties (e.g. Thomsen et al., 2007; Medialdea et al., 2014). In the above, we implicitly assumed that the dispersion observed in the beta dose recovery experiments is similar to the dispersion to be expected in a naturally well-bleached dose distribution of the same material. However, this is unlikely to be an accurate approach in samples that, for instance, were exposed to a heterogeneous environmental beta dose (e.g. Thomsen et al., 2007, Guérin et al., 2015). To investigate how sensitive our minimum dose estimates are to the size of the assigned additional uncertainty the additional uncertainty input parameter (a) was varied between 10 and 40%, i.e. varied over the range of over-dispersions commonly reported for well-bleached dose distributions (e.g. Arnold and Roberts, 2009). Fig. 5 shows how the estimated burial dose D_b (normalized to the value derived using a = 14%, as derived from the beta dose recovery experiments) varies as a function of a. For a given sample, all estimates of D_b are consistent with

each other although there is, as expected, a systematic increase in D_b with *a*. The average ratio of D_b calculated using an *a* value of 40% to that calculated using a value of 14% is 1.44±0.08 (n=5 samples).

5.3 SYNTHETIC ALIQUOT RESULTS

Although we focus on measurement of single-grains in this study, it is interesting to examine the doses that would have been measured using small multi-grain aliquots. Given the inherently low OSL sensitivity of these samples (few grains giving detectable OSL signals and most grains that are detectable have dim OSL signals), measurements of small multi-grain aliquots, each containing ~100 grains, might be expected to behave as single grains measurements, and so give dose distributions from which one could derive accurate deposition doses. As there was insufficient sample to undertake both single-grain and multi-grain measurements, we here examine the difference between these two approaches by combining the OSL signals from individual single-grain discs (each containing 100 single grains) to generate "synthetic" multi-grain aliquots. The synthetic multi-grain CAM_{UL} doses are given in Table 2; these range between 29 and 62 Gy and are very similar to the corresponding CAM_{UL} doses for the single-grain measurements (with the exception of sample ZT-2). However, none of these synthetic aliquots give doses smaller than 2 Gy and thus minimum dose modelling would significantly overestimate that of single-grain minimum dose modelling (see Table 2). Thus, despite of the low OSL sensitivity of these samples, multi-grain measurements (~100 grains per aliquot) are likely to produce significant overestimates of the burial age compared to those provided by true single-grain measurements.

6 AGES AND DISCUSSION

The resulting single-grain OSL ages are given in Table 2. The five weighted average (CAM_{UL}) ages range from 7 ±1 to 22 ±4 ka, similar to that from the synthetic multi-grain ages (13 ±3 to 24 ±4 ka) and to fine-grain IRSL and GLSL results reported by Lu et al., 2003. However, these average ages are affected by incomplete bleaching and thus significantly overestimate the burial age.

It is likely that minimum dose modelling of single-grain dose distributions provides a more accurate estimate of the burial dose. However, the calculated minimum doses from minimum dose modelling are dependent on the size of the assigned uncertainties (see Fig. 5). In the literature, it has often been argued that a "typical" over-dispersion for well-bleached samples is 15-20% (e.g. Arnold et al., 2008; Demuro et al., 2008; Turney et al., 2008), i.e. an additional uncertainty of 15-20% should be added to estimates of uncertainty based on intrinsic sources of variability (e.g. Poisson statistics, curve fitting errors etc.). Others (e.g. Thomsen et al., 2007; Medialdea et al., 2014; Sim et al., 2014) have argued that it would be more appropriate to use an additional uncertainty based on the over-dispersion determined in laboratory dose recovery experiments (preferably irradiated using a gamma source), although the latter approach presumably underestimates for samples exposed to significant dose rate heterogeneity during burial. However, Guérin et al. (2015) showed beta dose heterogeneity arising from non-uniform distribution of potassium in the sediment is of concern "*when the average grain size is in the sand and gravel range (rather than silt or clay), the potassium content is low (<1%), and the total dose rate is small (<1 Gy ka^{-1})*". Thus, at this stage, it is less likely that our samples are significantly affected by beta dose rate heterogeneity. In any case, based on the beta dose-recovery experiments, the minimum uncertainty with which an individual dose estimate can be known is 14 ±9%, although we acknowledge that this over-dispersion may be underestimated. Nonetheless, this minimum additional uncertainty

must be added (in quadrature) to the uncertainties assigned to individual dose estimates based on Poisson statistics and dose response curve fitting errors, if a true minimum estimate of uncertainty on individual single grain dose estimates is to be used in later analysis.

The minimum single-grain (IEU) ages (using an additional uncertainty of 14%, see Table 2) are all consistent with an average age of 320±25 y and there appears to be no stratigraphic relationship between ages of the samples. If an additional uncertainty of 40% is assumed, all IEU ages are consistent with an average age of 470±50 y. Thus, we conclude that these debris flow samples were all deposited in a short span of time (<100 years) within the last 500 years.

Giving the influence of insufficiently bleached grains on the OSL signal in these debris flows, the single-grain ages are much smaller than those from multi-grain measurements (Lu et al., 2003) and simulated multi-grain data. These debris flows were apparently deposited around 300-500 y ago, during the Little Ice Age in China (Zhu et al.,1973), which may indicate an association of debris flows in this area with cold periods or perhaps unstable periods of cold and warm fluctuation.

However, the importance of the anthropogenic-induced deterioration of the regional natural environment must also be considered. According to historical documents (Hou et al., 1985), significant deforestation in Xishan (Zhai Tang is in the Xishan mountain basin) in this period was associated with the Yuan Dynasty (AD 1271–1368) construction of a new capital in Beijing. Initially, a large amount of building construction material, and charcoal for cooking and heating, was taken from Xishan. Subsequently during the Ming Dynasty (AD 1368–1644), Beijing's increasing demand for raw materials continued the unsustained exploitation of the vegetation of the Xishan region. This was exacerbated by the increase in local population, which more than doubled from 300,000 to 670,000; this must also have increased pressure on agriculture. The resulting landscape degradation presumably led

to increased runoff; certainly there were frequent floods from ~650 to ~360 years ago in the Lugu (now Yongding) River, into which the Ma Lan Gou feeds (Hou et al., 1985). We deduce that the Zhai Tang debris flow deposits may represent geological evidence for the prolonged destruction of forest resources after the establishment of Yuan Dynasty capital in Beijing.

7 CONCLUSION

OSL dating of these debris flow deposits has proved challenging because of significant incomplete bleaching and the inherently low luminescence sensitivity of individual grains. Equivalent dose distributions are significantly positively skewed, with clearly identifiable leading edges at low doses. Using doses derived from simulated multi-grain data (synthetic aliquots) the ages of these deposits range between 13 ±3 and 24 ±4 ka, very similar to previously published fine-grain ages (Lu et al., 2003) and average single-grain ages. However, using single-grain dose distributions in combination with minimum dose modelling, the relative number of grains identified to be well-bleached range between 13 and 50%, strongly suggesting that multi-grain OSL techniques greatly overestimated the burial ages for these samples. We conclude that these debris flow samples were probably all deposited in a short span of time (<100 years) within the last 500 years, and tentatively associate these sediments with the historically-recorded catchment exploitation. Our results are of direct relevance to the assessment of mass movement hazard in the Men Tou Gou District, and we conclude that there is no evidence to suggest that the current risk of further debris flows has been mitigated.

393 ACKNOWLEDGEMENTS

394 This research was supported by the National Natural Science Foundation of China
395 (NSFC, Grant No. 40871017, 41602353, 41471007 and 41301006) and Social Science
396 Foundation of China (Grant No. 15CJY073). We are indebted to Yanyan Tian, Rui
397 Zhou, Hongyi Chen, Yugeng Liu and Jian Pan for assistance during field work. We
398 thank Shuzhen Peng and Min Ding for providing valuable comments on this
399 manuscript.

400

401 REFERENCES

402

403 Arnold, L.J., Roberts, R.G., Galbraith, R.F., Delong, S.B., 2009. A revised burial dose
404 estimation procedure for optical dating of young and modern-age sediments. Quat.
405 Geochronol. 4, 306-325.

406 Bøtter-Jensen, L., Andersen, C.E., Duller, G.A.T., Murray, A.S., 2003. Developments
407 in radiation, stimulation and observation facilities in luminescence measurements.
408 Radiat. Meas. 37, 535-541.

409 Bøtter-Jensen, L., Thomsen, K.J., Jain, M., 2010. Review of optically stimulated
410 luminescence (OSL) instrumental developments for retrospective dosimetry.
411 Radiat. Meas. 45, 253-257.

412 Cui, P., Liu, S.J., Tan, W.P., 2000. Progress of debris flow forecast in China. Journal
413 of Natural Disasters. 9 (2): 10-15 (in Chineses).

414 Cui, Z.J., 1996. Debris flow deposit and environment. China Ocean Press, Beijing, 1-
415 188 (in Chineses).

416 Duller, G.A.T., Bøtter-Jensen, L., Murray, A.S., Truscott, A.J., 1999. Single grain
417 laser luminescence (SGLL) mesurements using a novel automated reader. Nucl.
418 Instrum. Methods Phys. Res. B: Beam Interact. Mater. Atoms. 155(4), 506-514.

419 Duller, G.A.T., 2003. Distinguishing quartz and feldspar in single grain luminescence
420 measurements. Radiat. Meas. 37, 161-165.

421 Fuchs, M., Straub, J., Zöller, L., 2005. Residual luminescence signals of recent river
422 flood sediments: a comparison between quartz and feldspar of fine-and coarse-
423 grain sediments. Ancient TL. 23(1), 25-30.

Geach, M. R., Thomsen, K. J., Buylaert, J.-P., Murray, A. S., Mather, A. E., Telfer, M. W., 2015. Single-grain and multi-grain OSL dating of river terrace sediments in the Tabernas Basin, SE Spain. Quat. Geochron. 2015, 213-218.

Godfrey-Smith, D.I., Huntley, D.J., Chen, W.H., 1988. Optical dating studies of quartz and feldspar sediment extracts. Quat. Sci. Rev. 7(3~4), 373-380.

Guérin, G., Mercier, N., Adamiec, G., 2011. Dose-rate conversion factors: update. Ancient TL, 29, 5-8.

Guérin, G., Jain, M., Thomsen, K., Murray, A., Mercier, N., 2015. Modelling dose rate to single grains of quartz in well-sorted sand samples: the dispersion arising from the presence of potassium feldspars and implications for single grain OSL dating, Quaternary Geochronology, 27, 52-65.

Guérin, G., Combès, B., Lahaye, C., Thomsen, K.J., Tribolo, C., Urbanova, P., Guibert, P., Mercier, N., Valladas, H., 2015a. Testing the accuracy of a Bayesian central-dose model for single-grain OSL, using known-age samples. Radiation Measurements 81, 62-70

Guérin, G., Frouin, M., Talamo, S., Aldeias, V., Bruxelles, L., Chiotti, L., Dibble, H.L., Goldberg, P., Hublin, J.-J., Jain, M., Lahaye, C., Madelaine, S., Maureille, B., McPherron, S.P., Mercier, N., Murray, A.S., Sandgathe, D., Steele, T.E., Thomsen, K.J., Turq, A., 2015b. A multi-method luminescence dating of the Palaeolithic sequence of La Ferrassie based on new excavations adjacent to the La Ferrassie 1 and 2 Skeletons. J. Archaeol. Sci. 58, 147-166.

Guérin, G., Frouin, M., Tuquoi, J.; Thomsen, K.J., Goldberg, P., Aldeias, V., Lahaye, Ch., Mercier, N., Guibert P., Jain, M., Sandgathe, D., McPherron, S.P., Turq, A., Dibble, H.L., 2016. The complementarity of luminescence dating methods illustrated on the Mousterian sequence of the Roc de Marsal: A series of reindeer-dominated, Quina Mousterian layers dated to MIS 3. Quaternary International, in press.

451 Hansen, L., Funder, F., Murray, A.S., Mejdahl, V., 1999. Luminescence dating of the
452 last Weichselian Glacier advance in East Greenland. Quat. Sci. Rev. 18(2), 179-
453 190.

454 Hansen, V., Murray, AS., Buylaert, J-P., Yeo, E-Y., Thomsen, KJ. 2015. A new
455 irradiated quartz for beta source calibration. Radiation Measurements 81, 123–
456 127.

457 Hong, C,S., 1995. Occurrence and Countermeasures of debris flow in Beijing. Beijing
458 water conservancy. 4: 7-10.

459 Hou, R.Z., 1985. The Historical Atlas of Beijing. Beijing Press. pp. 127(in Chinese).

460 Jain, M., Murray, A.S., Bøtter-Jensen, L., 2003. Characterisation of blue-light
461 stimulated luminescence components in different quartz samples: implications for
462 dose measurement. Radiat. Meas. 37(4-5), 441-449.

463 Kristensen, J.A., Thomsen, K.J., Murray, A.S., Buylaert, J.P., Jain, M., Breuning-
464 Madsen, H., 2015. Quantification of termite bioturbation in a savannah ecosystem:
465 application of OSL dating. Quat. Geochronol. 30, 334-341.

466 Lapp, T., Jain, M., Thomsen, K.J., Murray, A.S., Buylaert, J.P., 2012. New
467 luminescence measurement facilities in retrospective dosimetry. Radiat. Meas.47,
468 803-808. 611-620.

469 Lu, Y.C., Wei, L.Y., Yin, J.H., Yin, G.M., Zhao, H., 2003. Dates and environments of
470 the Malan gravel formation as the torrent debris deposits along Qingshui River in
471 western hills, Beijing. Quaternary Sciences. 23(6), 611-620.

472 Medialdea, A., Thomsen, K.J., Murray, A.S., Benito, G., 2014. Reliability of
473 equivalent-dose determination and age-models in the OSL dating of historical and
474 modern palaeoflood sediments. Quat. Geochronol. 22, 11-24.

475 Mejdahl, V., 1987. Internal radioactivity in quartz and feldspar grains. Ancient TL. 5,

476 10-17.

477 Murray, A.S., Marten, R., Johnston, A., Martin, P., 1987. Analysis for naturally
478 occurring radionuclides at environmental concentrations by gamma spectrometry. J.
479 Radioanal. Nucl. Chem. 115(2), 263-288.

480 Murray, A.S., Wintle, A.G.,2000. Luminescence dating of quartz using an improved
481 single-aliquot regenerative-dose protocol. Radiat. Meas. 32, 57-73.

482 Murray, A.S., Wintle, A.G., 2003. The single aliquot regenerative dose protocol:
483 potential for improvements in reliability. Radiat. Meas. 47(9), 688-695.

484 Murray, A.S., Thomsen, K.J., Masuda, N., Buylaert, J.P., Jain, M., 2012. Identifying
485 well-bleached quartz using the different bleaching rates of quartz and feldspar
486 luminescence signals. Radiat. Meas. 47(9), 688-695.

487 Olley J.M., Caitcheon G.C., and Murray A.S., 1998. The distribution of apparent dose
488 as determined by optically stimulated luminescence in small aliquots of fluvial
489 quartz: implications for dating young sediments. Quaternary Science Reviews
490 (Quaternary Geochronology) 17, 1033-1040.

491 Prescott, J.R., Hutton, J.T., 1994. Cosmic ray contributions to dose rates for
492 luminescence and ESR: large depths and long-term time variations. Radiat. Meas.
493 23, 497-500.

494 Šilhán, K., Pánek, T., 2010. Fossil and recent debris flows in medium-high mountains
495 (Moravskoslezské Beskydy Mts, Czech Republic). Geomorphology. 124, 238-
496 249.

497 Sim, A.K., Thomsen, K.J., Murray, A.S., Jacobsen, G., Drysdale, R., Erskine, W.,
498 2014. Dating recent floodplain sediments in the Hawkesbury-Nepean river system
499 using single grain quartz OSL. Boreas,43(1), 1-21.

500 Thomsen, K. J., Murray, A. S., Bøtter-Jensen, L., Jungner, H., 2003. Variation with
501 depth of dose distributions in single grains of quartz extracted from an irradiated
502 concrete block. Radiation Measurements, 37 (4-5), 315-321.

503 Thomsen, K.J., Murray, A.S., Bøtter-Jensen, L., Kinahan, J., 2007. Determination of
504 burial dose in incompletely bleached fluvial samples using single grains of quartz.
505 Radiat. Meas. 42 (3), 370-379.

506 Thomsen K.J., Murray A., Jain M., 2012. The dose dependency of the over-dispersion
507 of quartz OSL single grain dose distributions. Radiation Measurements 47, 732-
508 739.

509 Thomsen, K. J., Murray, A. S., Buylaert, J. P., Jain, M., Hansen, J. H., Aubry, T.,
510 2016. Testing single-grain quartz OSL methods using sediment samples with
511 independent age control from the Bordes-Fitte rockshelter (Roches d'Abilly site,
512 central France). Quat. Geochron. 31, 77-96.

513 Wintle, A.G., 1973. Anomalous fading of thermoluminescence in mineral samples.
514 Nature. 245, 143-144.

515 Wintle, A.G., Murray, A.S., 2006. A review of quartz optically stimulated
516 luminescence characteristics and their relevance in single-aliquot regeneration
517 dating protocols. Radiat. Meas. 41, 369-391.

518 Wu, T. S., Jaiswal, M.K., Lin, Y.N., Chen, Y.W., Chen, Y.G., 2010. Residual
519 luminescence in modern debris flow deposits from western Taiwan: A single grain
520 approach. J Asian Earth Sci. 38, 274-282.

521 Xie, H., Zhong, D.L., Jin, H.C., 2001. Debris flow and landslide disasters control in
522 Mountain area of Beijing Cicy. Bulletin of Soil and Water Conservation.
523 21(3):37-45(In Chinese).

524 Xie, Y.Y., Cui, Z.J., 1992. Prevention and forecast of debris flow in Beijing mountain
525 area. Guizhou Science. 3, 132(In Chinese).

526 Zhao, B., Dong, G.Z., 1996. Mud-rock flows and its dangerous prediction in the
527 drainage area of the Qingshui River, Xishan Mt., Beijing. Geology of Beijing. 3:
528 1-14(In Chinese).

529 Zhao, Q., Thomsen, K.J., Murray, A.S., Wei, M., Pan, B., Song, B., Zhou, R., Chen,
530 S., Zhao, X., Chen, H., 2015. Testing the use of OSL from quartz grains for dating
531 debris flows in Miyun, northeast Beijing, China. Quaternary Geochronology. 30,
532 320-327.

533 Zhu, K.Z., 1873. A preliminary study on climate change in China in recent 5000
534 years. Science in China (B). 3(02): 115-120(In Chinese).

535

536 **Figure captions**

537

538

539 Figure 1: Location of the study site. (a) Regional map of study area. (b) Composite
540 section based on the four adjacent sampled sections illustrated in (c).

541

542 Figure 2: Multi-grain (~150 grains) quartz OSL characteristic for sample ZT-2
543 (preheat 200 ℃ for 10 s, cutheat 180 ℃). (a) Normalised luminescence
544 signals from calibration quartz (filled circle) and ZT-2 (open triangles).
545 (b) Representative dose response curve for sample ZT-2 showing
546 recycling and recuperation (open square and diamond symbols,
547 respectively) and the interpolation of the sensitivity-corrected natural
548 signal (filled circle) onto the dose response curve.

549

550 Figure 3: (a) Single-grain thermal transfer dose distribution for sample ZT-2. (b)-
551 (d) Single-grain beta dose recovery distribution for samples ZT-3 (given
552 dose of 3 Gy), ZT-1 (0.9 Gy) and ZT-4 (6 Gy), respectively.

553

554 Figure 4: Single-grain dose distributions (open symbols) for the five natural
555 samples. The natural test dose response (4.5 Gy) is shown as a function
556 of estimated dose. Filled symbols represents the grains identified by the
557 IEU model to be well-bleached using a dispersion value *a* of 0.14. The
558 insets show the same data for doses less than 19 Gy.

559

560 Figure 5: Variation of the estimated burial dose D_b (normalized to the value using
561 a = 14%) as a function of the additional uncertainty input parameter a.

562

563

Sample code	Depth (m)	w.c. (%)	Radionuclide (Bq/ kg)				Dose rate (Gy/ka)		
			U-238	Ra-226	Th-232	K-40	dry β	dry γ	Total
ZT-1	10	22	37 ± 15	27 ± 1.1	38.3 ± 1.2	527 ± 18	1.77 ± 0.07	1.06 ± 0.03	2.35 ± 0.14
ZT-2	9	10	27 ± 12	27 ± 0.9	41.1 ± 0.9	595 ± 18	1.91 ± 0.06	1.14 ± 0.03	2.61 ± 0.16
ZT-3	8	14	26 ± 15	31 ± 1.2	44.3 ± 1.2	574 ± 22	1.89 ± 0.08	1.19 ± 0.04	2.77 ± 0.18
ZT-4	3	26	33 ± 10	27 ± 0.8	42.3 ± 0.8	551 ± 13	1.84 ± 0.05	1.13 ± 0.03	2.22 ± 0.11
ZT-5	0.4	16	30 ± 17	27 ± 1.3	35.1 ± 1.4	466 ± 19	1.58 ± 0.08	0.97 ± 0.04	2.13 ± 0.12

Table1 Summary of depth, water content (w.c.), radionuclide concentrations and quartz dose rates for the four debris flow samples. Water content is taken as midway between observed and saturated water content. An internal quartz dose rate of 0.06±0.03 mGy a-1 has been assumed (Mejdahl, 1987). Total dose rate include cosmic rays and effect of water content.

Sample code	MG		SG								
	n_1	CAM_{UL} (Gy)	N	n_2	CAM_{UL} (Gy)	OD_{UL} (%)	$n_{w.b.14\%}$	IEU D_b (Gy)	$Age_{14\%}$ (a)	$n_{w.b.40\%}$	$Age_{40\%}$ (a)
ZT-1	17	41 ± 7	6500	63	37 ± 5	90 ± 15	9	0.8 ± 0.3	340 ± 140	9	490 ± 160
ZT-2	15	62 ± 8	4800	46	33 ± 6	98 ± 19	10	0.8 ± 0.3	320 ± 110	12	430 ± 150
ZT-3	17	52 ± 8	5800	47	60 ± 9	102 ± 18	6	0.9 ± 0.3	310 ± 120	7	620 ± 210
ZT-4	30	55 ± 5	6300	61	48 ± 5	65 ± 10	8	0.5 ± 0.3	240 ± 130	9	320 ± 140
ZT-5	20	29 ± 5	6000	56	15 ± 3	138 ± 29	28	0.8 ± 0.2	390 ± 70	36	510 ± 90

Table 2. Summary of synthetic multi-grain (MG) and single-grain (SG) results. 'MG' is simulated multi-grain measurements (i.e. synthetic aliquots, see text for details), 'SG' is single-grain measurements, 'n_1' is the number of accepted dose estimates from synthetic aliquots (i.e. summing of the single-grain data), 'N' is the number of measured single-grains, 'n_2' is the number of accepted dose estimates from single-grain data, '$n_{w.b.}$' is the number of grains identified to be well-bleached by the IEU minimum dose model using the given dispersion value *a* (see text for details), 'IEU D_b' is the burial dose estimated using the IEU and 'Age' is the age derived using the IEU D_b and the appropriate dose rate (see Table 1).

Fig.1

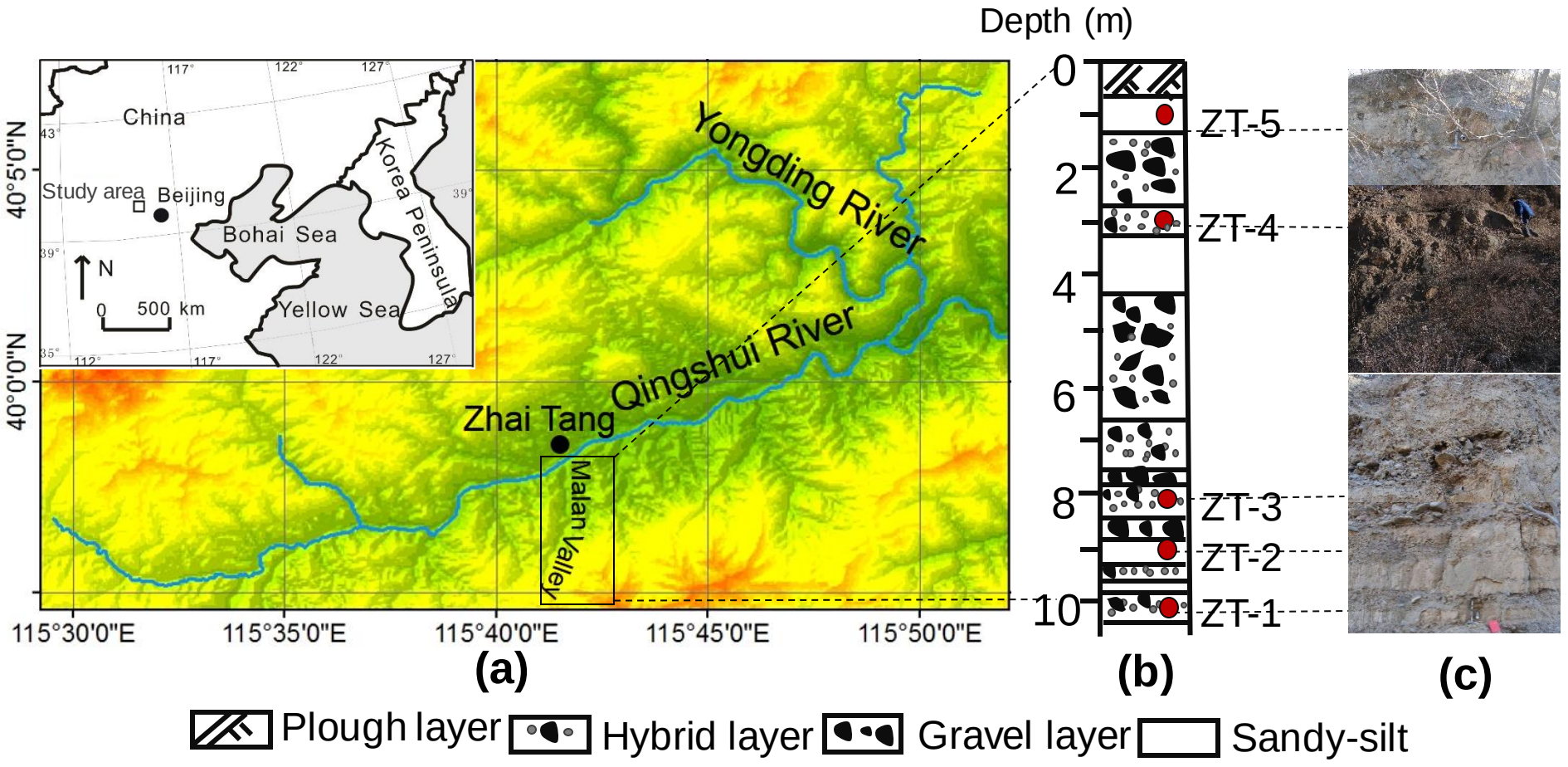
Depth (m)
China
Study area
Beijing
Bohai Sea
Korea Peninsula
Yellow Sea
N
0 500 km
Yongding River
Qingshui River
Zhai Tang
Malan Valley
40°5'0"N
40°0'0"N
115°30'0"E
115°35'0"E
115°40'0"E
115°45'0"E
115°50'0"E
0
2
4
6
8
10
ZT-5
ZT-4
ZT-3
ZT-2
ZT-1
(a)
(b)
(c)
Plough layer
Hybrid layer
Gravel layer
Sandy-silt

Fig.2

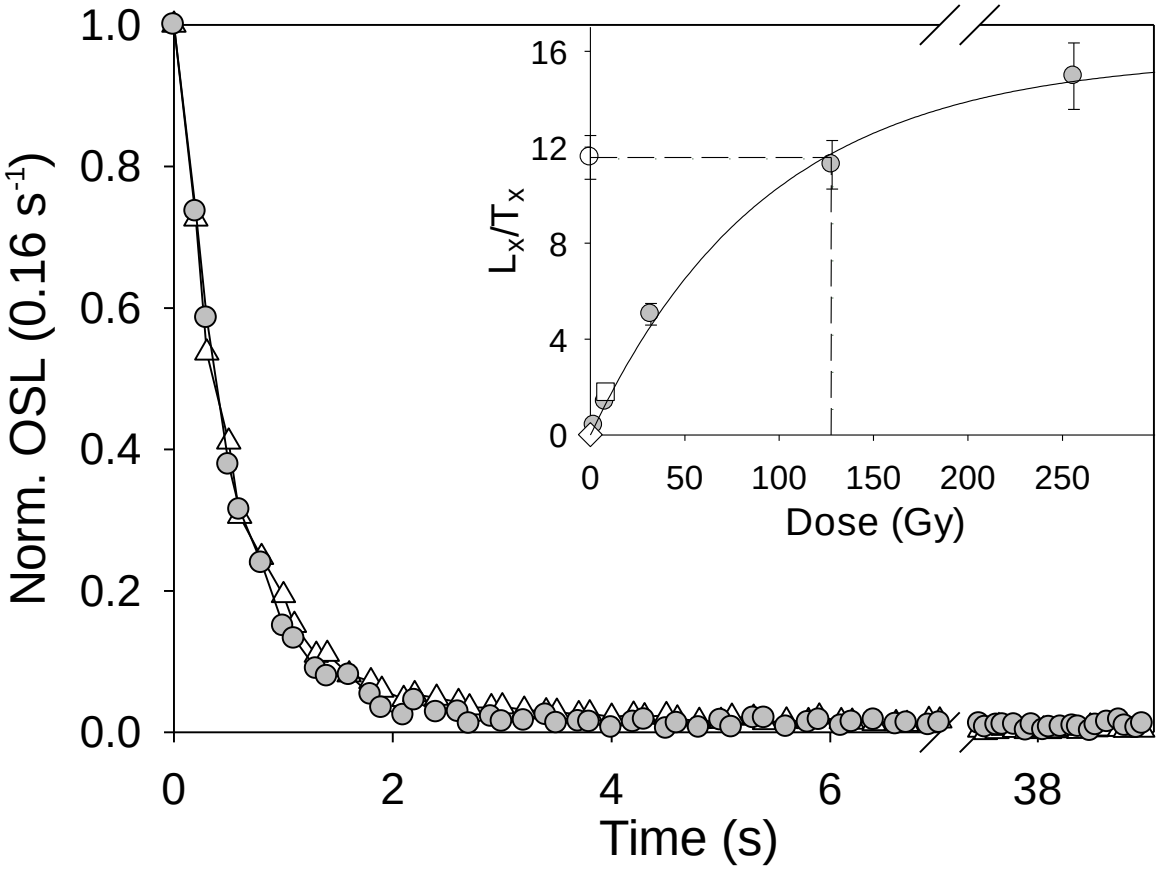
Norm. OSL (0.16 s-1)
1.0
0.8
0.6
0.4
0.2
0.0
0
2
4
6
38
Time (s)
Lx/Tx
16
12
8
4
0
0
50
100
150
200
250
Dose (Gy)

Fig.3

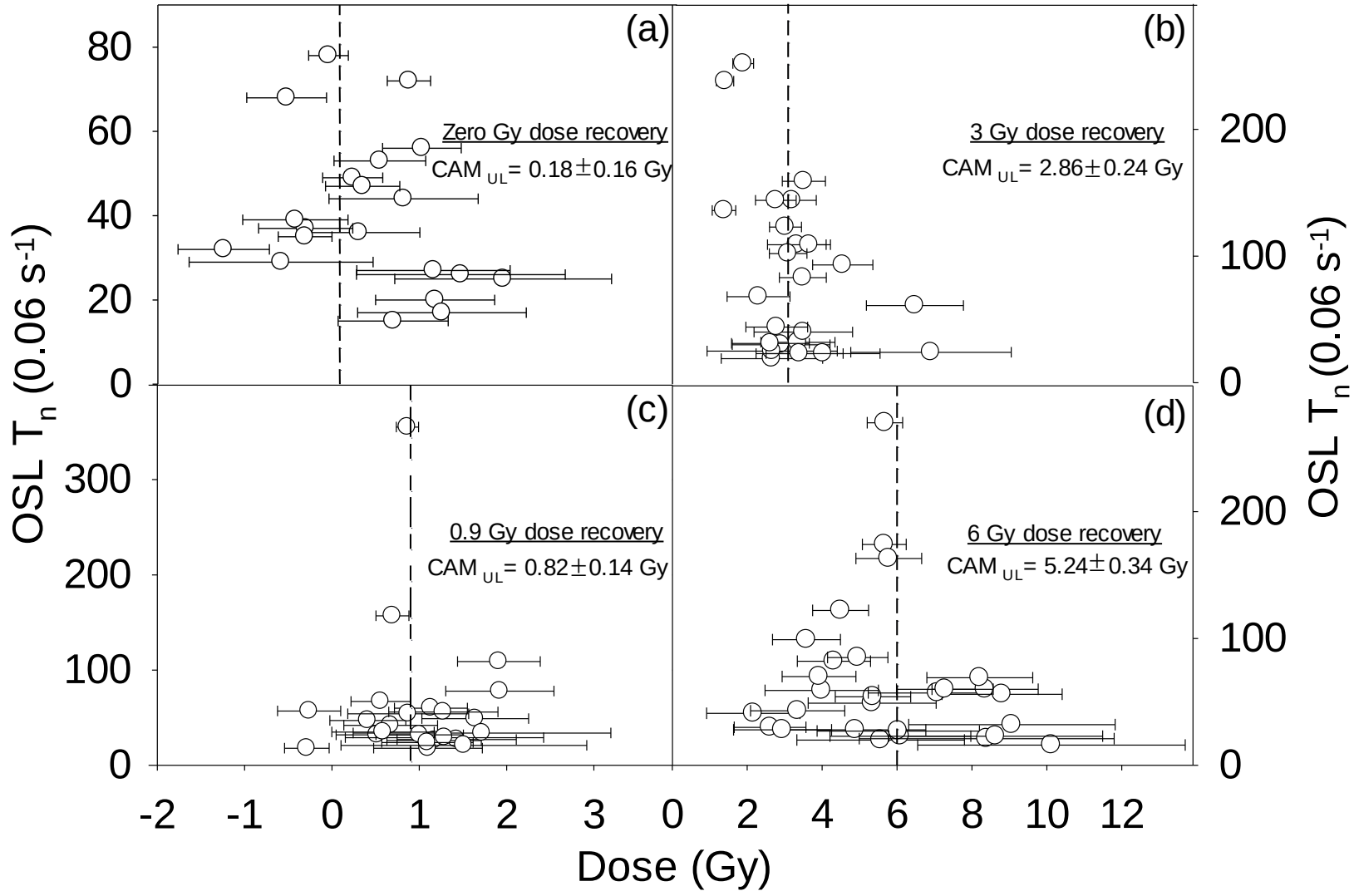
(a)
Zero Gy dose recovery
CAM UL= 0.18±0.16 Gy
(b)
3 Gy dose recovery
CAM UL= 2.86±0.24 Gy
(c)
0.9 Gy dose recovery
CAM UL= 0.82±0.14 Gy
(d)
6 Gy dose recovery
CAM UL= 5.24±0.34 Gy
OSL Tn (0.06 s-1)
OSL Tn (0.06 s-1)
Dose (Gy)
0
20
40
60
80
100
200
300
-2
-1
0
1
2
3
4
6
8
10
12

Fig.4

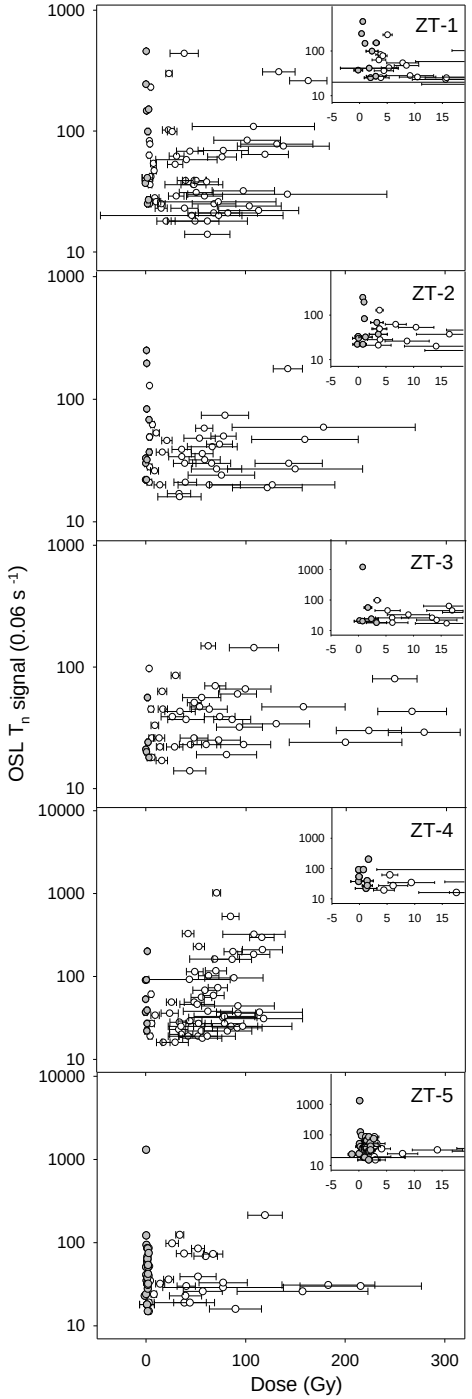

Fig.5

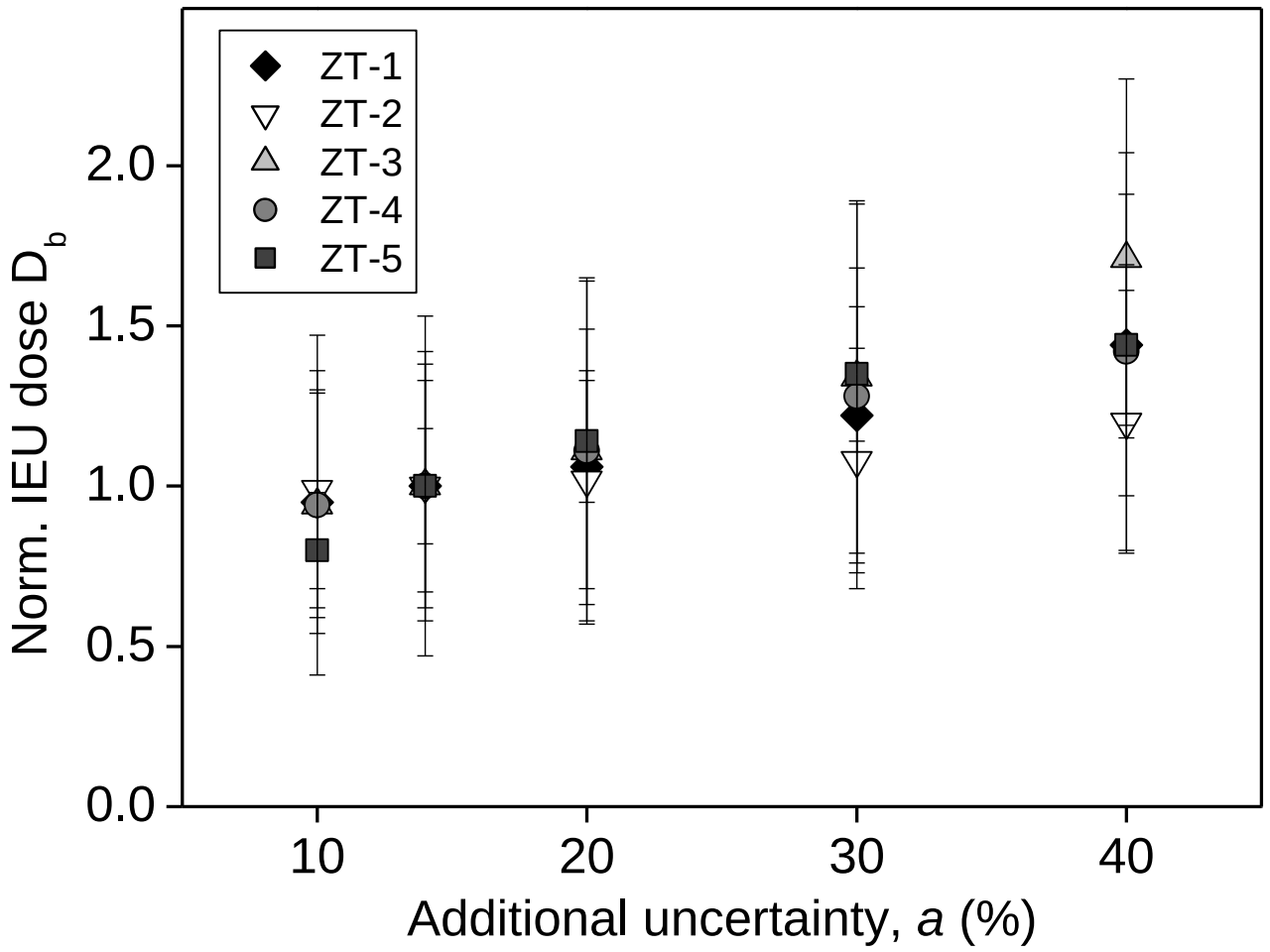
ZT-1
ZT-2
ZT-3
ZT-4
ZT-5
Norm. IEU dose D_b
2.0
1.5
1.0
0.5
0.0
10
20
30
40
Additional uncertainty, *a* (%)